1-2007

Short-term Response of Soil Iron to Nitrate Addition

Christopher J. Matocha
University of Kentucky, cjmato2@uky.edu

Mark S. Coyne
University of Kentucky, mark.coyne@uky.edu

Digital Object Identifier (DOI)
http://dx.doi.org/10.2136/sssaj2005.0170

Short-term Response of Soil Iron to Nitrate Addition

C. J. Matocha*
Department of Plant and Soil Science
Univ. of Kentucky
N-122 Agricultural Science Center-North
Lexington, KY 40546-0091

M. S. Coyne
Department of Plant and Soil Science
Univ. of Kentucky
N-122 Agricultural Science Center-North
Lexington, KY 40546-009

The inhibition of soil Fe(III) reduction by fertilizer NO_3^- applications is complex and not completely understood. This inhibition is important to study because of the potential impact on soil physicochemical properties. We investigated the effect of adding NO_3^- to a moderately well-drained agricultural soil (Sadler silt loam) under Fe(III)-reducing (anoxic) conditions. Stirred-batch experiments were conducted where NO_3^- was added (0.05 and 1 mM) to anoxic slurries and changes in dissolved Fe(II) and Fe(III), oxalate-extractable Fe(II), and dissolved NO_3^- were monitored as a function of time. Addition of 1 mM NO_3^- inhibited Fe(II) production sharply with reaction time, from 10% after 1 h to 85% after 24 h. The duration of inhibition in Fe(II) production was closely related to the presence of available NO_3^-, suggesting preferential use of NO_3^- by nitrate reductase enzyme. Active nitrate reductase was confirmed by the fivefold decline in NO_3^- reduction rates in the presence of tungstate (WO_4^{2-}), a well-known inhibitor of nitrate reductase. In addition, NO_3^-–dependent Fe(II) oxidation was observed to contribute to the inhibition in Fe(II) production. This finding was attributed to a combination of chemical reoxidation of Fe(II) by NO_2^-– and NO_3^-–dependent Fe(II) oxidation by autotrophic bacteria. These two processes became more important at a greater initial oxalate-Fe(II)/NO_3^- concentration ratio. The inhibitory effects in Fe(II) production were short-term in the sense that once NO_3^- was depleted, Fe(II) production resumed. These results underscore the complexity of the coupled N–Fe redox system in soils.

Abbreviations: AAS, atomic absorption spectrometry; HIV, hydroxy-interlayered vermiculite.

In oxic soil environments, Fe(III) is present in Fe(III) (hydr)oxide minerals or phyllosilicate clays. The importance of microbial Fe(III) reduction to Fe(II) is in part due to its impact on soil physicochemical properties (Stucki et al., 1996; Favre et al., 2002) and its role in organic C oxidation (Lovley, 2000). The reduction of Fe(III) can be inhibited by the presence of NO_3^-. This inhibition alters the speciation of transition metals such as Zn that adsorb to Fe(III) (hydr)oxide surfaces (Cooper et al., 2000). Four hypotheses have been proposed to explain the inhibitory mechanism of NO_3^- on Fe(III) reduction. The first hypothesis is based on thermodynamic arguments. The classical model of terminal electron-accepting processes that occur during microbial degradation of organic C predicts a sequence of oxidant consumption to follow the order of O_2 reduction, NO_3^- reduction, MnO_2 reduction, Fe(III) (hydr)oxide reduction, SO_4^{2-} reduction, and CH_4 production (McBride, 1994). Nitrate, due to its position on the redox ladder, increases the redox potential (E_H) beyond where Fe(III) reduction occurs (E_H = 200–400 mV), thereby preventing Fe(II) release (Ponnamperuma and Castro, 1964; Ponnamperuma, 1972). This view appears to be an oversimplification. It assumes that the more thermodynamically favorable reduction of NO_3^- excludes Fe(III) reduction, despite favorable thermodynamics in the latter reaction and variable reactivities of Fe(III) (hydr)oxide minerals (Roden, 2003). Furthermore, Munch and Ottow (1980) have pointed out that the activity of microbial reductases are more important than E_H in governing Fe(III) reduction.

The second hypothesis proposed by Ottow (1970) claimed that nitrate reductases, enzymes produced by bacteria to catalyze heterotrophic reduction of NO_3^- to NO_2^-, preferentially transfer electrons to NO_3^- rather than Fe(III). Sorensen (1982) suggested that nitrate reductase inhibited Fe(III) reduction because treatment of sediment slurries with 0.2 m*M* NO_3^- halted Fe(II) accumulation. After the NO_3^- supply was depleted, Fe(III) reduction resumed. Munch and Ottow (1980) pointed out that the presence of nitrate reductase is what leads to suppressed Fe(II) formation by NO_3^- under anoxic conditions. Nitrate reductases contain Mo in their active site that cycles between +4 (d^2) and +6 (d^0) oxidation states during reduction of NO_3^- to NO_2^- (Hille, 1996). Addition of WO_4^{2-} inactivates the enzyme by substitution for Mo (Scott et al., 1979; Smith, 1983). It may be possible to verify this hypothesis by adding WO_4^{2-} to soil slurries. To our knowledge, the effect of WO_4^{2-} on Fe(III) reduction is not known.

The third hypothesis involves concomitant reduction of NO_3^- and Fe(III) coupled to chemical reoxidation of Fe(II) by NO_2^-. In laboratory incubations of field soils, aquifer materials, and pure cultures, reduction of NO_3^- by nitrate reductase occurs simultaneously with Fe(III) reduction (Komatsu et al., 1978; Obuekwe et al., 1981; DiChristina, 1992; Broholm et al., 2000; Cooper et al., 2003). Under the scenario of concomitant Fe(III) and NO_3^- reduction, intermediates generated such as NO_2^- can transiently accumulate and chemically oxidize Fe(II) to Fe(III), leading to no net Fe(III) reduction (Lovley, 2000). This process has been proposed to occur in agricultural soil slurries and pure cultures (Komatsu et al., 1978; Obuekwe et al., 1981). However, DiChristina (1992) observed that neither NO_3^- nor NO_2^- behaved as chemical oxidants of Fe(II), but the inhibition was due to NO_2^- blocking electron transport to

Soil Sci. Soc. Am. J. 71:108-117
doi:10.2136/sssaj2005.0170
Received 1 June 2005.
*Corresponding author (cjmato2@uky.edu).

Fe(III) in pure cultures of *Shewanella putrafaciens*. The latter study was performed in the absence of mineral surfaces and Fe(III) salts were used as a source of Fe. In soil environments, it is conceivable that Fe(II) generated from Fe(III) reduction coordinates to mineral surfaces in an inner sphere complex or reprecipitates as a secondary Fe(II) mineral phase (Fredrickson et al., 1998; Zachara et al., 2002). The Fe(II) in these coordination environments, where O is the ligating atom, could be more reactive toward NO_2^- because the reduction potential is lowered for the Fe(III)–Fe(II) half-reaction (Luther et al., 1992). In fact, Sorensen and Thorling (1991) found that Fe(II) adsorbed on lepidocrocite [γ-$FeOOH_{(s)}$] reduced NO_2^- much more rapidly than dissolved, hexaaquo Fe(II).

The fourth hypothesis involves autotrophic bacteria that can reduce NO_3^- to N_2 with concomitant Fe(II) oxidation. These bacteria have been identified in European freshwater sediments (Straub et al., 1996), activated sludge treatment plants (Nielsen and Nielsen, 1998), urban lake sediments (Senn and Hemond, 2002), and anoxic rice paddy soil slurries (Klüber and Conrad, 1998). Dissolved Fe(II) and solid Fe(II) in minerals such as siderite [$FeCO_{3(s)}$] and magnetite [$Fe_3O_{4(s)}$] are capable of being used by bacteria during NO_3^- reduction (Straub et al., 1996; Weber et al., 2001). In addition, Fe(II) associated with phyllosilicate minerals has emerged as a suitable electron donor for autotrophs during NO_3^- reduction (Shelobolina et al., 2003).

Most of these studies evaluating the inhibitory effect of NO_3^- on Fe(III) reduction used pure cultures and synthetically prepared Fe(III) minerals or Fe(III) salts. This is due to the complexities associated with soil, where the inhibitory effect may be controlled in complex ways by these various processes that may compete with one another. The present study was undertaken to analyze the effect of NO_3^- addition on Fe(II) production in field soil subjected to anoxic [Fe(III)-reducing] conditions using stirred-batch experiments in the laboratory. Specifically, the objectives were to determine whether the effect of NO_3^- was due to: (i) competitive inhibition by nitrate reductase; (ii) concomitant reduction of Fe(III) and NO_3^- reduction linked to chemical reoxidation of biogenic Fe(II) by NO_2^-; or (iii) NO_3^--dependent Fe(II)-oxidizing autotrophic bacteria. Changes in different pools of Fe [dissolved Fe(II), oxalate-extractable Fe(II), and dissolved Fe(III)] and dissolved NO_3^- were monitored as a function of time and compared with controls (no NO_3^-). This will provide insight into the relative importance of the hypothetical pathways enumerated above. If the nitrate reductase competitive model is the main mechanism for inhibiting Fe(II) production, then addition of WO_4^{2-} should curtail the inhibition. Tungstate-treated soil slurries would also allow evaluation of the contribution of autotrophic Fe(II) oxidation coupled to NO_3^- reduction. This work will provide a better understanding of what happens when NO_3^- is surface applied as N fertilizer under Fe(III)-reducing conditions.

MATERIALS AND METHODS

Soil Collection

A Sadler silt loam (fine-silty, mixed, mesic Glossic Fragiudalf) was collected from the surface (0–5 cm) Ap horizon of a field site in Christian County, Kentucky. The soil developed in loess over sandstone parent materials and is moderately well drained (Karathanasis, 1987). Soil samples were taken with a cylindrical probe 2.0 cm in diameter from multiple soil cores (8–10) and placed in polyethylene bags. Preliminary extractions using oxalate and ferrozine revealed that Fe(II) was present at the time of sampling. Thus, the soil samples were immediately quick-frozen in the field using liquid N_2 to preserve the Fe(II) oxidation state and placed on dry ice during transport back to the laboratory. Samples were thawed, homogenized, carefully sieved to <2 mm, and stored under Ar in an O_2-free glove box (Coy Laboratory Products, Grass Lake, MI).

Soil Characterization

Part of the soil was removed from the anoxic chamber for characterization. Soil was separated into the following soil particle size separates: sand (2000–50 μm), silt (50–2 μm), and clay (<2 μm). Fractionation procedures followed those of Jackson (1974), using $NaHCO_3$ to disperse the soil and omitting chemical pretreatment steps. Chemical extractions were performed in triplicate on the whole soil and particle size fractions to quantify poorly crystalline Fe(III) (hydr)oxides (acid ammonium oxalate extraction, Phillips and Lovley, 1987), and total reducible Fe(III) (hydr)oxides (dithionite–citrate–bicarbonate extraction, Mehra and Jackson, 1960). Total Fe was measured in the extracts using atomic absorption spectrometry (AAS) (Shimadzu AA-6800, Kyoto, Japan). In addition, total Mn and Al were measured in the same extracts using AAS. Soil organic matter content was determined by loss-on-ignition (Nelson and Sommers, 1996) and total soil N by the Kjeldahl method (Bremner, 1996). Soil pH was determined in a 1:1 soil/solution ratio using deionized water and a pH meter (Metrohm 744, Herisau, Switzerland) with a combination glass electrode. Water extracts were collected to determine native concentrations of important anions (NO_3^-, NO_2^-, Cl^-, SO_4^{2-}, and PO_4^-) and cations (total Fe and total Mn). Results of chemical analyses were calculated on a dry-weight basis.

X-ray diffraction patterns were measured using a Siemens D-500 diffractometer with Cu Kα radiation and a current of 30 milliamps (Bruker AXS, Madison, WI). Intensities were recorded with a 0.05° step width and 1-s counting time per step. The powder method was used for the silt fraction and the scan range was 2 to 90° 2θ. Oriented slides were prepared using clay subsamples saturated with Mg, K, and Mg glycerol solvated and scanned from 2 to 30° 2θ. Cation exchange capacity was determined for the <2-μm fraction using Ca–Mg exchange.

A subsample of the <2-μm size fraction was examined using a Hitachi S-3200 scanning electron microscope equipped with a Noran Voyager energy dispersive x-ray spectrometer (Thermo Electron Corp., Waltham, MA) to better understand the chemical nature of Fe in the untreated clay fraction. The sample was prepared by sprinkling it on a C-covered sample stub attached to an Al holder that was sputter coated with Au–Pd.

Anoxic Stirred-Batch Experiments

Anoxic conditions were chosen to eliminate O_2 as a potential electron acceptor of Fe(II). All sample handling was conducted under an Ar atmosphere in a glove box to ensure anoxic conditions. Deionized water was purged for 3 h with high-purity Ar gas and transferred to the glove box for use in stirred-batch

experiments and preparation of solutions. Dissolved O_2 concentrations of Ar-deoxygenated water were measured periodically with a Clark-type polarographic electrode (Warner Instruments, Hamden, CT). Values ranged from 0.5 to 2 μmol L^{-1}, verifying anoxic conditions.

The <2-mm size fraction of the Sadler soil was used in five treatments (Table 1) of anoxic stirred-batch experiments. Experiments were prepared by adding 2 g of Sadler soil to a borosilicate glass serum bottle, after which 20 mL of Ar-deoxygenated water was added. The bottles were sealed with a rubber septum and allowed to prehydrate overnight. The reduction of NO_3^- was initiated by adding an aliquot of 1 *M* NO_3^- stock solution (prepared from a $NaNO_3$ salt) to a stirred soil suspension to achieve initial NO_3^- concentrations of 1000 and 50 μmol L^{-1}, corresponding to approximately 12 and 0.5 mmol kg^{-1} air-dried soil. These treatments are referred to as *high N* and *low N* (Table 1). Stirring was achieved using isotemp magnetic stir plates (Fisher Scientific, Hampton, NH) set to 350 rpm and experiments were conducted at room temperature (23–25°C). Suspension aliquots (1–2 mL) were withdrawn at 0.02, 1, 2, 4, 6, 8, and 24 h for high-N treatments and 0.02, 0.08, 0.17, 0.25, 0.5, 1, 1.5, 2, and 4 h for the low-N treatment. Sampling times for soil oxalate Fe(II) extractions were 0.02, 1, 4, and 24 h. Redox potential and pH were measured in soil slurries at 0, 4, and 24 h of reaction time.

We also studied the effect of adding WO_4^{2-} to inhibit production of active nitrate reductase (Scott et al., 1979; Smith, 1983). The purpose of inhibiting nitrate reductase was twofold: to evaluate contributions of the nitrate reductase competitive pathway and of the autotrophic pathway to inhibiting Fe(II) production. This treatment (high N–W) was identical to high N except Ar-deoxygenated water was added to the soil with 10 m*M* Na_2WO_4 (Table 1) and allowed to prehydrate overnight. Sampling times for high N–W were modified slightly because of slower NO_3^- reduction kinetics (see results below). To account for abiotic reactions, anoxic soil slurries were sterilized by autoclaving at 120°C (~138 kPa) for 30 min as described elsewhere (Tratnyek and Wolfe, 1993). Bottles were returned to the anoxic chamber and allowed to cool to room temperature before addition of 1000 μmol L^{-1} NO_3^-. The sterile treatment (high N–sterile) was otherwise treated identically to high N.

Control experiments (no added NO_3^-, Table 1) were reacted simultaneously with each series of treatments (high N, low N, high N–W, high N–sterile) to examine treatment-induced changes in Fe(II) and other soil properties (pH and E_H). When making comparisons among treatment controls, the controls were referred to as high-N control and high-N–W control, for example.

Additional experiments were conducted under anoxic conditions to include a range of initial NO_3^- concentrations (50, 100, 500, and 1000 μmol L^{-1}). Initial rates of NO_3^- removal were followed and fit to the Michaelis–Menten expression using nonlinear regression:

$$v = \frac{V_{max}[NO_3^-]}{K_m + [NO_3^-]} \quad [1]$$

where v is the initial rate of NO_3^- removal (mmol L^{-1} min^{-1}), V_{max} is the estimated maximum rate (mmol L^{-1} min^{-1}), and K_m is the affinity constant for the substrate (μmol L^{-1}). The K_m value corresponds to the NO_3^- concentration at which the rate reaches half the maximum rate. Thus, a smaller K_m represents a stronger affinity between enzyme and substrate.

Chemical Analysis of Stirred-Batch Samples

Slurry aliquots were passed through a 0.2-μm membrane filter. Filtrates were immediately mixed with ferrozine [3-(2-pyridyl)-5,6-diphenyl-1,2,4-triazine-4′, 4″-disulfonic acid monosodium salt] buffered to pH 5.5 with MES [2-(*N*-morpholino)ethanesulfonic acid monohydrate] to complex dissolved Fe(II). Absorbance spectra of the Fe(II)–ferrozine complex were recorded at 562 nm (Stookey, 1970) in Suprasil quartz cuvettes (Hereaus Optics, Buford, GA) with a 1-cm optical pathlength at 24°C on a double-beam Shimadzu UV-3101PC spectrophotometer (Kyoto, Japan) against appropriate standards. The estimated method detection limit is 0.5 μmol L^{-1} in a 1-cm cell. Total Fe concentrations in ferrozine solutions were measured using AAS. The difference between total Fe and Fe(II) was used to estimate dissolved Fe(III). Total Mn concentrations in the filtrates were measured using AAS.

Nitrate and NO_2^- in filtrates were quantified by ion chromatography with conductivity detection using a Metrohm 792 Basic IC with a MetroSep A column and MetroSep RP guard disc holder and a 3.2 mmol L^{-1} Na_2CO_3/1 mmol L^{-1} HCO_3^- eluent (Metrohm, Houston, TX). Typical retention times for NO_2^- and NO_3^- were 6 and 9 min. In some cases, orthophosphate and SO_4^{2-} were quantified at 11.6 and 13.1 min, respectively. The indophenol blue method was used for quantification of NH_4^+ on the remaining sample filtrates uncomplexed with ferrozine (Weatherburn, 1967). The redox potential was measured with a Metrohm combination Pt electrode with an Ag–AgCl reference electrode and corrected to the standard H electrode by adding 199 mV (Patrick et al., 1996). Total alkalinity in water extracts of control bottles was determined by titration with standardized 0.05 *M* HCl.

The acid ammonium oxalate extraction (0.2 *M* at pH 3) described by Phillips and Lovley (1987) was used to extract solid-phase Fe(II). The method targets reduced Fe(II) phases such as magnetite [$Fe_3O_{4(s)}$] and siderite [$FeCO_{3(s)}$] and poorly crystalline Fe(III) minerals (Van Bodegom et al., 2003). An oxalate extraction would also remove adsorbed Fe(II). Soil slurry aliquots, between 0.1 and 0.5 mL, were pipetted into 20-mL glass serum bottles and combined with oxalate. Bottles were sealed with butyl rubber stoppers and Al crimp caps and shaken for 24 h in the dark. Bottles

Table 1. Description of the treatments imposed for anoxic stirred-batch experiments.

Objective	Treatment designation	Description
Follow NO_3^- reduction and Fe(II) consumption	high N	1 m*M* NO_3^- + anoxic soil
Effect of lowering NO_3^- conc.	low N	0.005 m*M* NO_3^- + anoxic soil
Inhibit NO_3^- reductase	high N–W	1 m*M* NO_3^- + anoxic soil + 10 m*M* WO_4^{2-}
Account for abiotic reactions	high N–sterile	1 m*M* NO_3^- + autoclaved anoxic soil
Measure Fe(II) in absence of NO_3^-	control	no added NO_3^-

were decapped and suspensions were filtered through 0.2-μm membrane filters. An aliquot of filtrate was combined with ferrozine and pH 5.5 MES buffer and Fe(II) was quantified as described above. Because the percentage change in Fe(III) during the experiments was small compared with the total Fe(III) already present in the soil (see below), it was decided to express the values as Fe(II) to avoid uncertainty in the data. The inhibition percentage of Fe(II) production was calculated as described in DiChristina (1992):

$$\text{inhibition percentage} = \left\{1 - \left[\frac{\text{Fe(II)}_{\text{treatment}}}{\text{Fe(II)}_{\text{control}}}\right]\right\}100 \quad [2]$$

The sum of dissolved Fe(II) and oxalate-extractable Fe(II) concentrations for each treatment and its control represented the values for $Fe(II)_{treatment}$ and $Fe(II)_{control}$, respectively.

Geochemical modeling was used to assess possible Fe(II) solid phases such as siderite and magnetite that may form by computing saturation indices [SI = log(ion activity product/solubility product constant)] with MINEQL+ (Schecher, 1998). Precipitation is favored when SI > 0, indicating that solutions are supersaturated with respect to the mineral. SI values <0 indicate that solutions are undersaturated with respect to precipitation of the mineral.

RESULTS

Untreated Soil Characteristics

The Sadler soil contains 22% sand, 67% silt, and 11% clay. The soil had an initial pH of 7.1 and total organic C and N values of 13 and 1.2 g kg^{-1}. Initial NO_3^- and SO_4^{2-} concentrations in water extracts were 11 ± 4 and 17 ± 5 μ*M*, respectively. The whole soil, silt, and clay fractions contained oxalate-extractable Fe/Na dithionite–citrate–bicarbonate (DCB)-extractable Fe ratios of 0.33, 0.32, and 0.47 (Table 2). This suggests the presence of crystalline Fe(III) oxides (Schwertmann and Cornell, 1991); however, these extractants will also chemically reduce structural Fe(III) from phyllosilicate minerals (Roth et al., 1969; Komadel et al., 1990). Quartz was the predominant mineral identified in the silt fraction, with a trace of feldspar, based on x-ray diffraction (XRD) analysis. The clay fraction, which accounted for only 11% of the dry weight of the soil, contributed 36 and 56% of the total oxalate- and DCB-extractable Fe (Table 2). Thus, the chemistry and mineralogy of this fraction was studied further.

Mineralogy of the clay (<2-μm) fraction was mixed and dominated by hydroxy-interlayered vermiculite (HIV) and kaolinite. The HIV was identified in the Mg-saturated sample by the 1.3-nm XRD peak, which failed to expand on glycerol treatment and collapsed to 1.0 nm in the K-saturated sample at 550°C (Fig. 1a). The presence of kaolinite was confirmed by the disappearance of the 0.7-nm peak at 550°C in the K-saturated sample. Quartz was present based on diagnostic d-spacings at 0.33 and 0.42 nm (not shown). The measured cation exchange capacity of the clay fraction was 39 ± 11 $cmol_c$ kg^{-1}, consistent with low-charge kaolinite and steric blockage of interlayer charge sites by the hydroxyl interlayer in HIV (Barnhisel and Bertsch, 1989). Representative scanning electron microscope (SEM) micrographs of the clay size fraction showed that Fe was associated with phyllosilicate minerals. Particles with platy morphology and diameters that were 2 to 3 μm were common and typified by relative Si/Al ratios of 1.75 (Fig. 1b). These findings, in combination with the considerable oxalate-extractable Al (Table 2), are consistent with HIV containing Al interlayers. A peak at 6.4 keV in the energy dispersive spectra was identified as the kα feature of Fe. Iron could be present as a structural cation in the octahedral sheet of HIV, in agreement with published average structural chemical formulas for HIV (Barnhisel and Bertsch, 1989). Discrete Fe(III) (oxy)hydroxides were not detected by XRD or SEM in the clay fraction. This suggests that they are either absent or below detection limits.

Anoxic Control Experiments

The reduction of Fe(III) in high-N control soil slurries was evident based on Fe(II) accumulation in the dissolved and oxalate-extractable pools (Fig. 2a and 2b). The concentration of oxalate-extractable Fe(II) produced was only a small fraction of the total oxalate-extractable Fe (Fe_{ox} in Table 2), indicating that a majority of the Fe still remained as Fe(III). The measured redox potential (E_H) in control bottles for both high N and high N–W verified that conditions were Fe(III) reducing (Table 3). The rise in soil pH is consistent with bioreduction of soil Fe(III) (Table 3) due to proton consumption (Munch and Ottow,1980).

In general, Fe(II) production in the oxalate-extractable fraction was at least 10 times greater than the dissolved Fe(II) fraction (Fig. 2a,b). This suggests that as Fe(III) reduction proceeds, the released Fe(II) reprecipitates as solid Fe(II) minerals (Fredrickson et al., 1998; Zachara et al., 2002) or resorbs to the soil (Kukkadapu et al., 2001). Regarding the former scenario, thermodynamic modeling indicated that solutions were supersaturated with respect to siderite precipitation based on SI values >1 in all treatments and controls (Table 3). Siderite is a common secondary product of crystalline and poorly crystalline Fe(III) (hydr)oxide reduction (Fredrickson et al., 1998; Lovley, 2000; Zachara et al., 2002). In our calculations, it was assumed that the carbonate required for $FeCO_{3(s)}$ precipitation originated from the alkalinity generated (as measured by titration in control bottles) during microbial decomposition of organic C coupled to dissimilatory Fe(III) reduction under anoxic conditions (Suess, 1979). As pointed out by Zachara

Table 2. Chemical characterization of the Sadler silt loam soil and size fractions†.

Fraction	Fe_{DCB}	Mn_{DCB}	Al_{DCB}	Fe_{ox}	Mn_{ox}	Al_{ox}
	mmol kg^{-1}					
Whole soil	157 (6.4)‡	15.0 (2)	52.3 (1)	53.2 (4)	12.2 (1.2)	ND§
Sand	20.9 (12.6)	2.95 (2.4)	8.2 (4.4)	9.9 (2.4)	1.28 (0.4)	6.4 (0.7)
Silt	25.7 (2.3)	1.81 (0.1)	21.6 (3.6)	38.2 (32.2)	2.35 (0.2)	11.4 (9.4)
Clay	58.7 (0.1)	3.43 (0.2)	21.7 (1.2)	26.5 (5.6)	10.2 (3.3)	74.0 (6.7)

† Fe_{DCB}, Al_{DCB}, and Mn_{DCB} (dithionite–citrate–bicarbonate-extractable Fe, Al, and Mn, respectively) were extracted according to Mehra and Jackson (1960); Al_{ox}, Fe_{ox}, and Mn_{ox} (oxalate-extractable Fe, Al, and Mn, respectively) extracted according to Phillips and Lovley (1987).

‡ Values in parentheses represent one standard deviation from the mean.

§ ND = not determined.

et al. (2002), siderite precipitation can occur biologically and abiologically, with the latter possibly occurring at a faster rate.

A factor that could potentially inhibit Fe(II) production is the presence of Mn(III,IV) oxide minerals (Table 2). Manganese(III,IV) oxide minerals that persist under the reducing conditions encountered here in a state of redox disequilibrium could react with Fe(II), producing Fe(III) (Hyacinthe et al., 2001). If this occurred, then an increase in dissolved Mn and a decrease in dissolved Fe(II) would be expected. Total dissolved Mn in control bottles remained constant (data not shown) and dissolved Fe(II) increased (Fig. 2a), ruling out this possibility.

Impact of Nitrate on Iron(II) Production

Results of the high-N experiments are shown in Fig. 2. The addition of 1000 μmol L^{-1} NO_3^- (~12.5 mmol kg^{-1}) inhibited Fe(II) production in both the oxalate-extractable and dissolved fractions (Fig. 2a and 2b). The inhibitory effects increased sharply with time, from 10% after 1 h to 85% after 24 h (Table 4). Dissolved Fe(III) production was accelerated in the high-N treatments, generally greater than the control with an apparent plateau reached after ~6 h (Fig. 2c). In contrast, there was a small but noticeable decrease in dissolved Fe(III) in the control bottles, corresponding to conditions that became more reducing during the experiments (Table 3).

The inhibition of Fe(II) production coincided with reduction of NO_3^-, which was reduced at a rate of 0.68 (± 0.06) mmol kg^{-1} h^{-1} (R^2 = 0.99, p < 0.001; Fig. 2d). No NO_2^- was detected as an intermediate and only slight increases in NH_4^+ were observed, accounting for only ~5% of the reduced NO_3^- (data not shown).

The predominantly biological nature of NO_3^- reduction was shown by the sensitivity toward autoclaving (Fig. 2d, high N–sterile). Additional evidence in support of a biological reduction of NO_3^- was found in the saturation behavior shown by NO_3^-. Nitrate reduction was described well by Michaelis–Menten kinetics (r^2 = 0.99; Fig. 3). The affinity constant K_m value derived from the fit of Eq. [1] to the data in Fig. 3 was 70 μmol L^{-1} NO_3^- and V_{max} was 1.2 μmol L^{-1} NO_3^- min^{-1}.

Results where the initial NO_3^- concentration was lowered (low N) are shown in Fig. 4. There was an immediate inhibition in Fe(II) production of 66% after 1 h where most of the NO_3^- was reduced (Fig. 4a and 4b, Table 4). The rate of NO_3^- reduction was 0.3 (±0.02) mmol kg^{-1} h^{-1}. After NO_3^- depletion, Fe(III) reduction resumed in the low-N slurries. This was shown by the drop in Fe(II) inhibition at 4 and 24 h (Table 4).

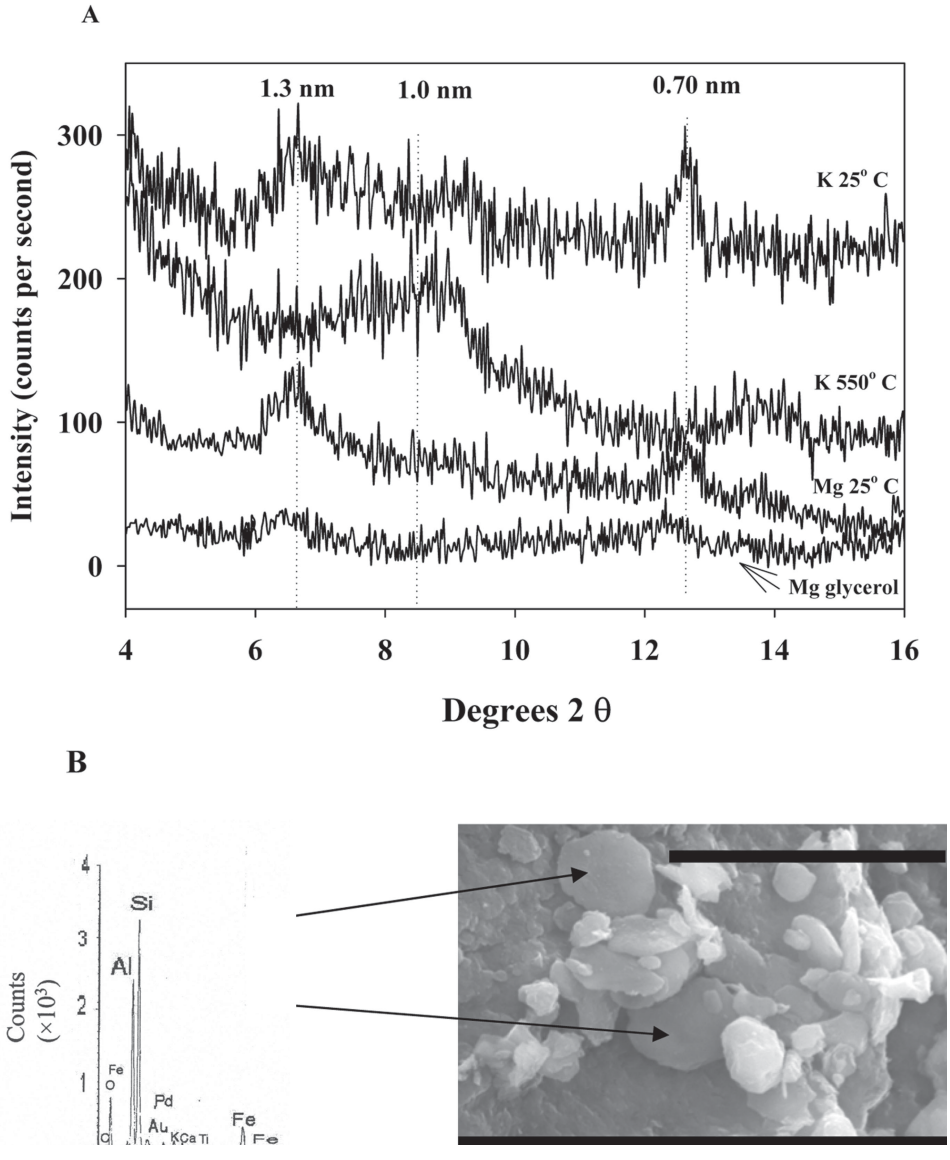

Fig. 1. (A) X-ray diffraction patterns of the clay fraction after Mg saturation at 25°C, Mg-glycerol solvation at 25°C, K saturation at 25°C, and K saturation at 550°C; (B) representative scanning electron micrograph of the clay fraction. The energy dispersive x-ray spectrum shown corresponds to the platy particle indicated by the arrows. The Au and Pd were a result of the coating process. Scale bar equals 5 μm and no peaks were detected beyond 10 keV.

Effect of Tungstate on Nitrate Reduction and Iron(II) Production

The response of NO_3^- reduction and Fe(II) production to added WO_4^{2-} in soil slurries is shown in Fig. 5. It appears that WO_4^{2-} elicited inhibitory effects on Fe(III) reduction based on three- to fourfold less oxalate-extractable Fe(II) in high-N–W control slurries than their high-N control counterparts at the outset of the reactions (compare Fig. 5b and Fig. 2b). As a result, introduction of NO_3^- in soil slurries treated with WO_4^{2-} (high N–W) resulted in a different inhibition pattern than the high-N treatment (Fig. 5a and 5b). The greatest inhibition in Fe(II) production was observed during the first 4 h of reaction, followed by only

a slight inhibition at 24 h (Table 4). It is possible that this early inhibition of Fe(II) production arose from cells taking time to build new electron transport chains to use Fe(III) as an electron acceptor now that NO_3^- was blocked. No clear trend was evident in dissolved Fe(III) in response to NO_3^- addition (Fig. 5c).

The rate of NO_3^- reduction in high N–W (Fig. 5d) was 0.14 (±0.01) mmol kg^{-1} h^{-1} (R^2 = 0.99, $p < 0.001$). This rate was approximately fivefold less than the high-N experiments and twofold less than the low-N treatment.

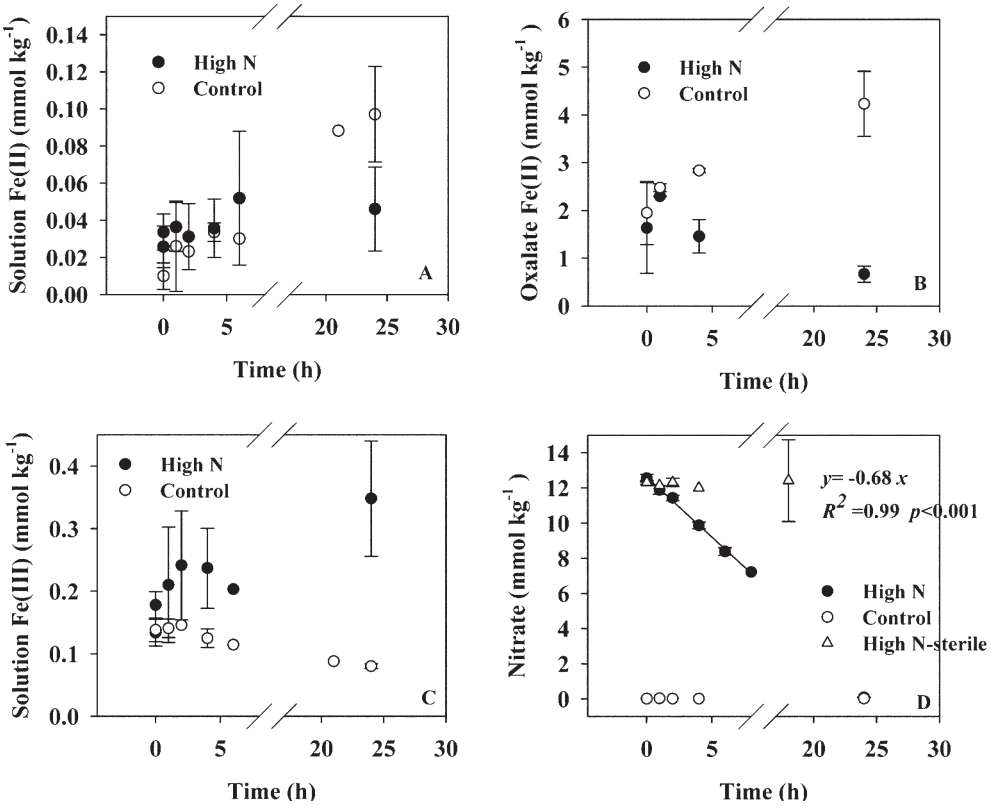

Fig. 2. Time course of (A) solution Fe(II), (B) oxalate-extractable Fe(II), (C) solution Fe(III), and (D) solution NO_3^- for the high-N treatment and high-N control soil slurries. The solution NO_3^- values for high-N–sterile are plotted in (D). Error bars represent the standard deviation from the mean for duplicate or triplicate runs.

DISCUSSION

Inhibition of Soil Iron(II) Production by Nitrate Reductase

As already mentioned, several hypothetical pathways have been proposed to explain the mechanism of the suppression of Fe(II) production following addition of NO_3^-. Inhibition of Fe(II) production cannot be explained by an increase in E_H in high-N and high-N–W experiments (Table 4). Although the variability was high, E_H values never rose above −100 mV during the course of the reaction for high-N and high-N–W soil slurries (Table 3). All values were well within the Fe(III)-reducing zone (Patrick et al., 1996) and did not increase to positive potentials (200–400 mV) as suggested elsewhere (Ponnamperuma and Castro, 1964; Ponnamperuma, 1972) to explain the inhibition of Fe(II) production by NO_3^-. Similarly, Klüber and Conrad (1998) reported no change in redox potential due to addition of 1000 μmol L^{-1} NO_3^- to anoxic rice (*Oryza sativa* L.) paddy soil slurries. The pH values tended to increase with reaction time in high N, high N–W, and their controls (Table 3). This suggests that changes in pH or E_H were not responsible for the inhibitory effects in Fe(II) production.

According to the nitrate reductase competitive model (second hypothesis), NO_3^- would be preferentially used as an electron acceptor. Once all the NO_3^- was reduced, then Fe(III) would be used as an electron acceptor and Fe(II) production would resume (Munch and Ottow, 1980; Sorensen, 1982). In the high-N experiments, the inhibition in Fe(II) production increased >70% from 1 to 24 h as NO_3^- was being reduced (Fig. 2a, 2b, and 2d, Table 4). Iron(II) production resumed after 48 h subsequent to complete NO_3^- depletion (data not shown). At low initial NO_3^- concentrations (low N), the maximum in Fe(II) inhibition occurred

Table 3. The pH, reduction potential (E_H), and calculated saturation indices (SI)† for predicted Fe(II) mineral solids in high-N and high-N–W treatments and their controls.

Treatment	pH			E_H			SI‡			
							Siderite		Magnetite	
	0 h	4 h	24 h	0 h	4 h	24 h	0 h	24 h	0 h	24 h
					mV					
High N	7.8(0.1)§	7.5(0.3)	8.2(0.1)	−113(25)	−154(5)	−151(50)	1.8	2.5	−59	−66
High N control	7.8(0.1)	7.6(0.1)	7.9(0.1)	−129(6)	−206(7)	−162(37)	1.7	1.9	−59	−61
High N–W	7.6(0.2)	7.7(0.03)	7.9(0.1)	−124(15)	−126(11)	−145(15)	2.1	2.7	−58	−60
High N–W control	7.7(0.2)	ND¶	8.1(0.1)	−160(36)	ND	−145(39)	1.9	2.6	−59	−66

† Determined using MINEQL+ (Schecher, 1998). Input data included alkalinity, dissolved Fe(II), dissolved Fe(III), pH, and E_H.

‡ Log ion activity product/solubility product constant.

§ Values in parentheses represent one standard deviation from the mean.

¶ ND = not determined.

Table 4. Inhibition percentage in Fe(II) production and contribution of Fe(II) oxidation to NO_3^- reduction in high-N, high-N–W, and low-N treatments.

Treatment	Inhibition of Fe(II) production			Fe(II) oxidation by NO_3^-†		
	1 h	4 h	24 h	1 h	4 h	24 h
High N	10(0.1)‡	62(2)	85(3)	8(0.1)	10(3)	6(1)
Low N	66(2)	53(2)	0§	87(11)	51(7)	0
High N–W	56(17)	72(10)	5(4)	0	16(6)	0

† Determined assuming NO_3^- was reduced to N_2, and by subtracting measured Fe(II) (oxalate-extractable + dissolved) for each treatment from the control.

‡ Values in parentheses represent one standard deviation from the mean.

§ Values of 0 represent points where Fe(II) production has resumed or where negligible NO_3^- has been reduced.

earlier than in the high-N treatment (Fig. 4a and 4b, Table 4). The production of Fe(II) clearly resumed after complete NO_3^- reduction in low-N treatments (Fig. 4a and 4b). These results agree with Sorensen (1982), who found that Fe(II) production commenced only after complete reduction of 200 μmol L^{-1} NO_3^- in anoxic slurries. Munch and Ottow (1980) argued that NO_3^- will inhibit Fe(II) production in soils due to the direct action of nitrate reductase.

It was expected that addition of WO_4^{2-} would curtail Fe(II) inhibition if the nitrate reductase competitive model is the main mechanism involved. Iron(II) inhibition continued in the high-N–W experiments (Table 4); however, this trend was confounded by the unanticipated effect of WO_4^{2-} on Fe(III) reduction as much less oxalate-extractable Fe(II) was initially present in high-N–W control slurries than high-N controls (compare Fig. 5b and Fig. 2b). Nonetheless, the pronounced decrease in the NO_3^- reduction rate from 0.68 mmol kg^{-1} h^{-1} in the high-N slurries (Fig. 2d) to 0.14 mmol kg^{-1} h^{-1} in the high-N–W treatment (Fig. 5d) indicates active nitrate reductase in our system. Molybdoenzymes of *E. coli* were inactivated by similar levels of WO_4^{2-}, resulting in a drastic decline in nitrate reductase activity (Scott et al., 1979; Smith, 1983). In addition, negligible NO_3^- reduction in the high-N–sterile treatment (Fig. 2d) further substantiates the important role of nitrate reductase, which is inactivated by autoclaving (Sorensen, 1982).

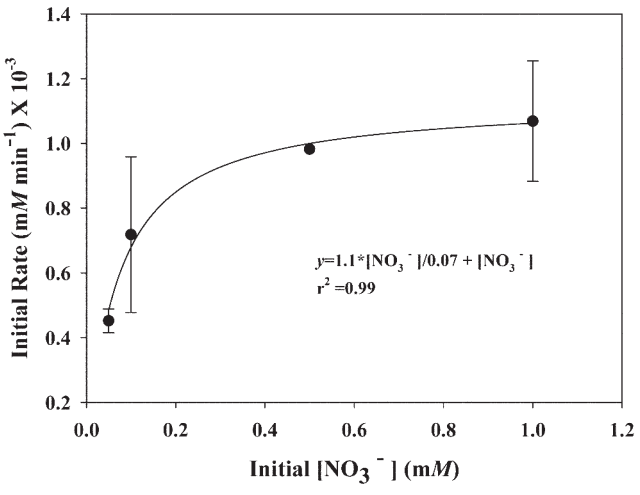

Fig. 3. Michaelis–Menten kinetic plot in anoxic soil slurries of the Sadler silt loam. The line is a nonlinear fit of the Michaelis–Menten equation to the data. Error bars represent the standard deviation from the mean for duplicate or triplicate runs.

The saturation behavior displayed in NO_3^- reduction rates (Fig. 3) further supports a biological reduction of NO_3^- by the nitrate reductase enzyme. This has been ascribed to limiting soil organic C concentrations for heterotrophic denitrifiers (Bowman and Focht, 1974; Kohl et al., 1976). This could have been the case in our experimental systems because no C additions were made and the native soil organic C level was used (~1.3%). The apparent K_m value (70 μmol L^{-1} NO_3^-) was lower than that reported elsewhere (Bowman and Focht, 1974; Kohl et al., 1976), suggesting greater affinity of NO_3^- in our soil. This could reflect differences in soil organic C availability, soil type, and experimental conditions.

It is conceivable that NO_3^- consumption was also due to Fe(III)-reducing bacteria that are able to simultaneously reduce NO_3^- and Fe(III), with a preference toward NO_3^- (DiChristina, 1992; Krause and Nealson, 1997). Several *Geobacter* species have been shown to reduce NO_3^- (Coates et al., 1996; Senko and Stolz, 2001) without the involvement of Mo-containing enzyme systems based on sustained nitrate reductase activity in the presence of up to 2 × 10^4 μmol L^{-1} WO_4^{2-} (Murillo et al., 1999).

Inhibitory Effects due to Concomitant Iron(III) and Nitrate Reduction Coupled to Iron(II)

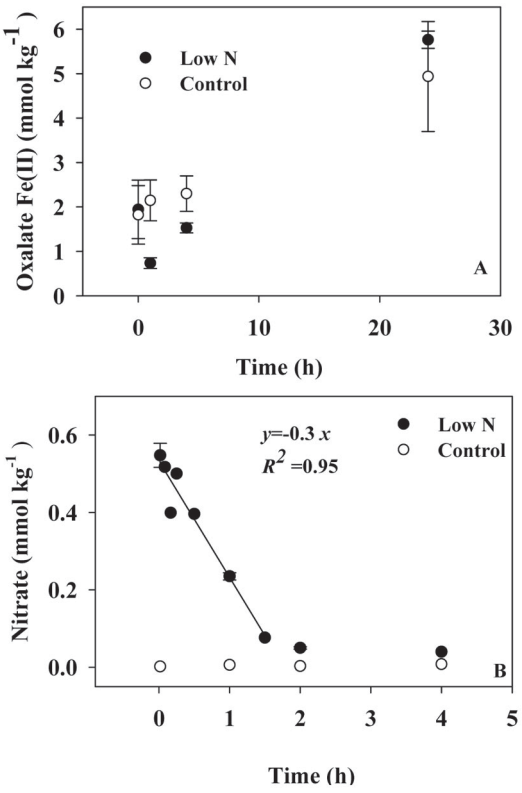

Fig. 4. Time course of (A) oxalate-extractable Fe(II), and (B) solution NO_3^- for the low-N treatment and low-N control soil slurries. Error bars represent the standard deviation from the mean for duplicate or triplicate runs.

Reoxidation by Nitrite

If NO_3^- functioned strictly as an inhibitor of Fe(III) reduction by nitrate reductase, then one would expect Fe(II) levels to remain constant during NO_3^- reduction as pointed out by Obuekwe et al. (1981) and observed in sediment slurries by Sorensen (1982). In our studies, however, Fe(II) levels in both dissolved and oxalate-extractable fractions were not constant during the NO_3^- reduction process, but dropped below the corresponding controls. Inhibition of Fe(II) production in high N and low N was most pronounced whenever NO_3^- was still present in solution (Fig. 2a, 2b, 2d, 4a, and 4b, Table 4). These results indicate that Fe(II) was oxidized during NO_3^- reduction and contributed to inhibiting Fe(II) production. The contributions of Fe(II) oxidation to NO_3^- reduction were 6 to 10% in the high-N and 50 to 90% in the low-N slurries (Table 4). Additional support for Fe(II) oxidation was based on the greater levels of dissolved Fe(III) produced in high-N treatments when compared with the high-N control (Fig. 2c). This evidence indicates that the nitrate reductase competitive model was not the only mechanism operating in the inhibition of Fe(II) formation by NO_3^-.

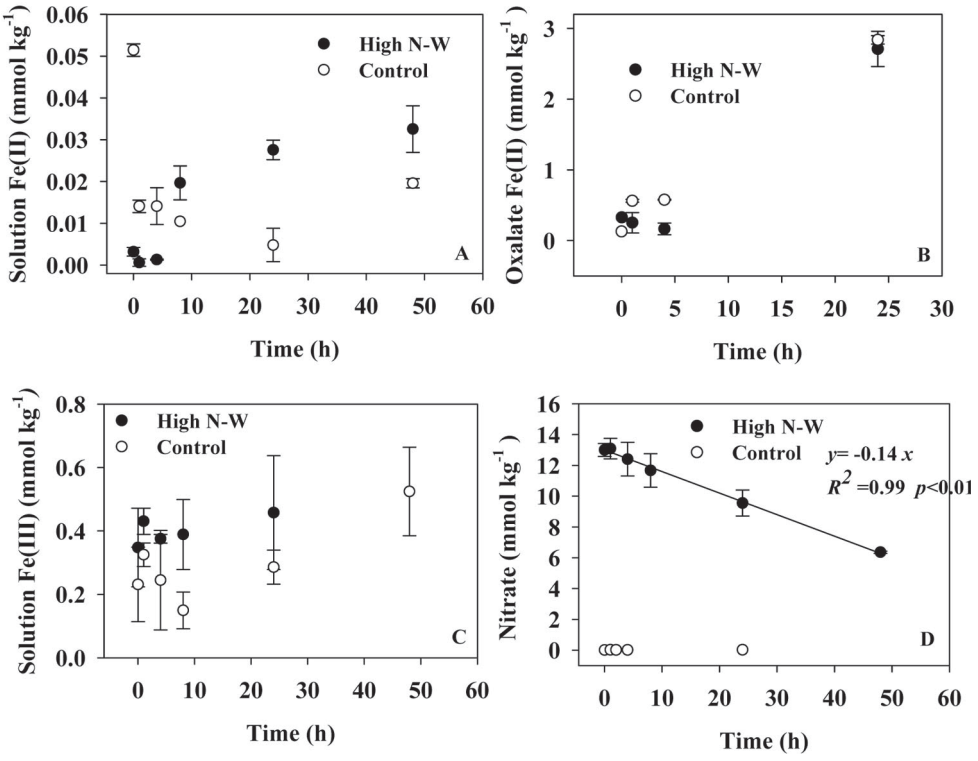

Fig. 5. Time course of (A) solution Fe(II), (B) oxalate-extractable Fe(II), (C) solution Fe(III), and (D) solution NO_3^- for high-N–W treatment and high-N–W control soil slurries. Error bars represent the standard deviation from the mean for duplicate or triplicate runs.

Iron(II) production in control bottles did not appear to level off during our experiments, suggesting that microbial Fe(III) reduction was proceeding at the time when NO_3^- was added (Fig. 2a, 2b, 4a, and 4b). Secondary reactions involving chemical Fe(II) reoxidation by NO_2^- formed during concomitant Fe(III) and NO_3^- reduction may explain the inhibitory effects in Fe(II) production (Komatsu et al., 1978; Obuekwe et al., 1981). The greatest contribution of Fe(II) oxidation to NO_3^- reduction was found in the low-N slurries (Table 4). This may be ascribed to the initial stoichiometric excess of oxalate-extractable Fe(II) over NO_3^- (3.5:1) in this treatment (Fig. 4a and 4b), whereas in high-N experiments, the ratio was 0.2:1 (Fig. 2b and 2d). This would provide more available Fe(II) to chemically react with NO_2^- produced as an intermediate during heterotrophic reduction of NO_3^-. Nitrite is a versatile ligand in that it can coordinate to a metal via the N or O atoms, with bonding on the N forming a stronger complex (Shriver et al., 1994).

One possible form of reactive Fe(II) that may chemically reduce NO_2^- in our soil systems is $FeCO_{3(s)}$ (Table 3). Using data compiled by Bard et al. (1985), one can compute a favorable thermodynamic driving force for oxidation of siderite by NO_2^- to poorly crystalline Fe(III) hydroxide ($\Delta G°_r$ = -128 kJ mol^{-1}):

$$NO_2^- + 3FeCO_3(s) + 7H_2O \rightarrow 3Fe(OH)_3(s) + \tfrac{1}{2}N_2 + 3HCO_3^- + 2H^+ \quad [3]$$

It is not clear whether the overall reaction in Eq. [3] occurs at a rate relevant to our time series data. The importance of siderite oxidation by NO_2^- as a possible pathway in inhibiting Fe(II) production merits further study.

Another form of Fe(II) that may be present in our systems is adsorbed Fe(II). A wide variety of sorption sites in the Sadler soil [kaolinite, HIV, and possibly Fe(III) (hydr)oxide minerals] would be available for Fe(II) at pH values encountered in this study (Table 3). For example, Kukkadapu et al. (2001) reported that Fe(II) produced during biological reduction of a sediment-derived clay fraction resorbed to kaolinite. Adsorbed Fe(II) as an inner sphere complex to oxo functional groups is a strong chemical reductant, reflected by a lowered reduction potential when compared with dissolved Fe(II) (Wehrli, 1990; Luther et al., 1992). Nitrite is known to be heterogeneously reduced by adsorbed Fe(II) forms, at estimated rates of ~1 to 3.5 μmol L^{-1} NO_2^- min^{-1} at pH 8 (Van Cleemput and Baert, 1983; Sorensen and Thorling, 1991). These rates are generally faster than the rate of NO_3^- reduction in our studies (0.2–1 μmol L^{-1} NO_3^- min^{-1}, Fig. 2d and 4d), and may explain why NO_2^- was not detected as an intermediate. These reactive forms of Fe(II) may have been rapidly oxidized to Fe(III) by NO_2^- and may explain the inhibition in Fe(II) production.

Inhibitory Effects due to Autotrophic, Nitrate-Dependent Iron(II) Oxidation

Autotrophic bacteria may also be responsible for the inhibiting effect of NO_3^- on Fe(II) production by coupling

NO_3^- reduction to Fe(II) oxidation (Straub et al., 1996). In our experiments, the immediate oxidation of Fe(II) following NO_3^- addition resulted in accelerated production of dissolved Fe(III) in high-N slurries (Fig. 2a–2d). The dissolved Fe(III) is probably chelated by dissolved organic matter. Although Fe(II) oxidation could also be due to the chemical pathway mentioned above, no loss of NO_3^- was noted in the high-N–sterile slurries (Fig. 2d), nor was the production of Fe(III) (data not shown). Klüber and Conrad (1998) reported immediate production of Fe(III) coupled to NO_3^- reduction under anoxic conditions and attributed this finding to bacterial Fe(II) oxidation. Enrichment cultures of NO_3^--dependent Fe(II) oxidizers produce poorly crystalline ferrihydrite [$Fe(OH)_{3(s)}$] as the primary product of Fe(II) oxidation (Straub et al., 1996).

The Fe(II) used by NO_3^--dependent Fe(II) oxidizers may originate from dissolved Fe(II) (Straub et al., 1996) or possibly siderite (Weber et al., 2001). In addition, structural Fe(III) in HIV (Fig. 1) that is reduced may provide the available Fe(II). Interestingly, a recent study showed that structural Fe(II) in smectite was available as an electron donor to support autotrophic Fe(II) oxidation by NO_3^- (Shelobolina et al., 2003). The structural Fe(II) to Fe(III) conversions mediated by bacteria occurred without the Fe being detached from the smectite.

It was expected that blocking nitrate reductase with WO_4^{2-} (high-N–W experiments) would isolate the contribution of the Fe(II)-oxidizing, NO_3^--dependent autotrophic pathway. This would allow Fe(III) reduction to proceed and produce Fe(II), which then could participate in autotrophic NO_3^- reduction (Straub et al., 1996). As mentioned above, added WO_4^{2-} affected Fe(III) reductase and may explain the discrepancy between NO_3^- reduced and Fe(II) oxidized in high-N–W slurries (Fig. 5b and 5d, Table 4). Past studies have shown that inhibitors such as WO_4^{2-} have the potential to impact nontarget microorganisms when added to sediments (Oremland et al., 1989).

SUMMARY AND CONCLUSIONS

It has long been known that fertilizer NO_3^- applications to flooded soil can result in N loss through denitrification. Our results show that soil Fe(III) reduction can be hindered as well and may result in temporary changes in soil physicochemical properties if NO_3^- fertilizer is added to Fe(III)-reducing soil. Addition of NO_3^- to soil under Fe(III)-reducing (anoxic) conditions inhibited Fe(II) production by preferential use of NO_3^- by nitrate reductase and anoxic Fe(II) oxidation. Processes that account for anoxic Fe(II) oxidation include concomitant Fe(III) and NO_3^- reduction coupled to reoxidation of Fe(II) by NO_2^- and NO_3^--dependent, autotrophic Fe(II) oxidation. The role of these two processes in the inhibition in Fe(II) production became more important at high initial oxalate-extractable Fe(II) and NO_3^- concentrations. Thus, it may be important to consider the initial ratios of extractable Fe(II) to NO_3^- when trying to explain the mechanism of inhibition in Fe(II) production in anoxic soil environments. The inhibition was short-term in the sense that once NO_3^- was depleted, Fe(II) production resumed. An important consequence of NO_3^--dependent Fe(II) oxidation is that the dissolved Fe(III) produced, even at micromolar levels, could behave as a kinetically labile oxidant.

It is difficult to separate the contributions of anoxic Fe(II) oxidation between NO_3^--dependent, autotrophic Fe(II) oxidation and chemical reoxidation of Fe(II) by NO_2^- during concomitant Fe(III) and NO_3^- reduction on the basis of our data. One approach could include a prolonged incubation to exhaust microbially reducible Fe(III). Once Fe(II) production has stabilized, NO_3^- could be added to isolate Fe(II) oxidation. Perhaps addition of ferrozine to soil slurries to rapidly complex Fe(II) before NO_2^- oxidizes it would allow one to distinguish between chemical and biological processes. Furthermore, it would be interesting to follow Fe(II) and Fe(III) changes in the clay fraction to identify reactive species.

ACKNOWLEDGMENTS

This project was supported by National Research Initiative Competitive Grant no. 2002-35107-12214 from the USDA Cooperative State Research, Education, and Extension Service. We thank Larry Rice at ASTECC for assistance in SEM-EDS analysis and L.W. Murdock for help in acquiring the soil.

REFERENCES

Bard, A.J., R. Parsons, and J. Jordan. 1985. Standard potentials in aqueous solution. Marcel Dekker, New York.

Barnhisel, R.I., and P.M. Bertsch. 1989. Chlorites and hydroxyl-interlayered vermiculite and smecite. p. 729–788. *In* J.B. Dixon and S.B. Weed (ed.). Minerals in soil environments. 2nd ed. SSSA Book Ser. 1. Madison, WI.

Bowman, R.A., and D.D. Focht. 1974. The influence of glucose and nitrate concentrations upon denitrification rates in sandy soils. Soil Biol. Biochem. 6:297–301.

Bremner, J.M. 1996. Nitrogen—Total. p. 1085–1121. *In* D.L. Sparks (ed.) Methods of soil analysis. Part 3. SSSA Book Ser. 5. SSSA, Madison, WI.

Broholm, M.M., C. Crouzet, E. Arvin, and C. Mouvet. 2000. Concurrent nitrate and Fe(III) reduction during anaerobic biodegradation of phenols in a sandstone aquifer. J. Contam. Hydrol. 44:275–300.

Coates, J.D., D.J. Lonergan, H. Jenter, and D.R. Lovley. 1996. Isolation of *Geobacter* species from a variety of sedimentary environments. Appl. Environ. Microbiol. 62:1531–1536.

Cooper, D.C., F. Picardal, J. Rivera, and C. Talbot. 2000. Zinc immobilization and magnetite formation via ferric oxide reduction by *Shewanella putrefaciens 200*. Environ. Sci. Technol. 34:100–106.

Cooper, D.C., F.W. Picardal, A. Schimmelmann, and A.J. Coby. 2003. Chemical and biological interactions during nitrate and goethite reduction by *Shewanella putrefaciens 200*. Appl. Environ. Microbiol. 69:3517–3525.

DiChristina, T.J. 1992. Effects of nitrate and nitrite on dissimilatory iron reduction by *Shewanella putrefaciens 200*. J. Bacteriol. 174:1891–1896.

Favre, F., D. Tessier, M. Abdelmoula, J.M. Génin, W.P. Gates, and P. Boivin. 2002. Iron reduction and changes in cation exchange capacity in intermittently waterlogged soil. Eur. J. Soil Sci. 53:175–183.

Fredrickson, J.K., J.M. Zachara, D.W. Kennedy, H. Dong, T.C. Onstott, N.W. Hinman, and S. Li. 1998. Biogenic iron mineralization accompanying the dissimilatory reduction of hydrous ferric oxide by a groundwater bacterium. Geochim. Cosmochim. Acta 62:3239–3257.

Hille, R. 1996. The mononuclear molybdenum enzymes. Chem. Rev. 96:2757–2816.

Hyacinthe, C., P. Anschutz, P. Carbonel, J.M. Jouanneau, and F.J. Jorrisen. 2001. Early diagenetic processes in the muddy sediments of the Bay of Biscay. Mar. Geol. 177:111–128.

Jackson, M.L. 1974. Soil chemical analysis—Advanced course. M.L. Jackson, Madison, WI.

Karathanasis, A.D. 1987. Mineral solubility relationships in Fragiudalfs of western Kentucky. Soil Sci. Soc. Am. J. 51:474–481.

Klüber, H.D., and R. Conrad. 1998. Effects of nitrate, nitrite, NO, and N_2O on methanogenesis and other redox processes in anoxic rice field soil. FEMS Microbiol. Ecol. 25:301–318.

Kohl, D.H., F. Vithayathil, P. Whitlow, G. Shearer, and S.H. Chien. 1976. Denitrification kinetics in soil systems: The significance of good fits of data to mathematical forms. Soil Sci. Soc. Am. J. 40:249–253.

Komadel, P., P.R. Lear, and J.W. Stucki. 1990. Reduction and reoxidation of nontronite: Extent of reduction and reaction rates. Clays Clay Miner. 38:203–208.

Komatsu, Y., M. Takagi, and M. Yamaguchi. 1978. Participation of iron in denitrification in waterlogged soil. Soil Biol. Biochem. 10:21–26.

Krause, B., and K.H. Nealson. 1997. Physiology and enzymology involved in denitrification by *Shewanella putrefaciens*. Appl. Environ. Microbiol. 63:2613–2618.

Kukkadapu, R.K., J.M. Zachara, S.C. Smith, J.K. Fredrickson, and C. Liu. 2001. Dissimilatory bacterial reduction of Al-substituted goethite in subsurface sediments. Geochim. Cosmochim. Acta 65:2913–2924.

Lovley, D.R. 2000. Fe(III) and Mn(IV) reduction. p. 3–30. *In* D.R. Lovley (ed.) Environmental microbe–metal interactions. ASM Press, Washington, DC.

Luther, G.W., III, J.E. Kostka, T.M. Church, B. Sulzberger, and W. Stumm. 1992. Seasonal iron cycling in the salt marsh sedimentary environment—The importance of ligand complexes with Fe(II) and Fe(III) in the dissolution of Fe(III) minerals and pyrite, respectively. Mar. Chem. 40:81–103.

McBride, M.B. 1994. Environmental chemistry of soils. Oxford Univ. Press, New York.

Mehra, O.P., and M.L. Jackson. 1960. Iron oxide removal from soils and clays by a dithionite–citrate system buffered with sodium bicarbonate. Clays Clay Miner. 7:317–327.

Munch, J.C., and J.C.G. Ottow. 1980. Preferential reduction of amorphous to crystalline iron oxides by bacterial activity. Soil Sci. 129:15–21.

Murillo, F.M., T. Gugliuzza, J. Senko, P. Basu, and J.F. Stolz. 1999. A heme-C-containing enzyme complex that exhibits nitrate and nitrite reductase activity from the dissimilatory iron-reducing bacterium *Geobacter metallireducens*. Arch. Microbiol. 172:313–320.

Nelson, D.W., and L.E. Sommers. 1996. Total carbon, organic carbon, and organic matter. p. 961–1010. *In* D.L. Sparks (ed.) Methods of soil analysis. Part 3. SSSA Book Ser. 5. SSSA, Madison, WI.

Nielsen, J.L., and P.H. Nielsen. 1998. Microbial nitrate-dependent oxidation of ferrous iron in activated sludge. Environ. Sci. Technol. 32:3556–3561.

Obuekwe, C.D., D.W.S. Westlake, and F.D. Cook. 1981. Effect of nitrate on reduction of ferric iron by a bacterium isolated from crude oil. Can. J. Microbiol. 27:692–697.

Oremland, R.S., J.T. Hollibaugh, A.S. Maest, T.S. Presser, L.G. Miller, and C.W. Culbertson. 1989. Selenate reduction to elemental selenium by anaerobic bacteria in sediments and culture: Biogeochemical significance of a novel, sulfate-independent respiration. Appl. Environ. Microbiol. 55:2333–2343.

Ottow, J.C.G. 1970. Selection, characterization, and iron-reducing capacity of nitrate reductaseless (*nit*$^-$) mutants from iron-reducing bacteria. Z. Allg. Mikrobiol. 8:441–443.

Patrick, W.H., R.P. Gambrell, and S.P. Faulkner. 1996. Redox measurements of soils. p. 1255–1273. *In* D.L. Sparks (ed.) Methods of soil analysis. Part 3. SSSA Book Ser. 5. SSSA, Madison, WI.

Phillips, E.J.P., and D.R. Lovley. 1987. Determination of Fe(III) and Fe(II) in oxalate extracts of sediment. Soil Sci. Soc. Am. J. 51:938–941.

Ponnamperuma, F.N. 1972. The chemistry of submerged soils. Adv. Agron. 24:29–96.

Ponnamperuma, F.N., and R.U. Castro. 1964. Redox systems in submerged soils. Int. Congr. Soil Sci. Trans. 8:379–386.

Roden, E.E. 2003. Fe(III) oxide reactivity toward biological versus chemical reduction. Environ. Sci. Technol. 37:1319–1324.

Roth, C.B., M.L. Jackson, and J.K. Syers. 1969. Deferration effect on structural ferrous–ferric iron ratio and CEC of vermiculites and soils. Clays Clay Miner. 17:253–264.

Schecher, W. 1998. MINEQL+ Version 4.5. Environ. Res. Software, Hallowell, ME.

Schwertmann, U., and R.M. Cornell. 1991. Iron oxides in the laboratory: Preparation and characterization. Wiley-VEH, New York.

Scott, R.H., G.T. Sperl, and J.A. DeMoss. 1979. *In vitro* incorporation of molybdate into demolybdoproteins in *Escherichia coli*. J. Bacteriol. 137:719–726.

Senko, J.M., and J.F. Stolz. 2001. Evidence for iron-dependent nitrate respiration in the dissimilatory iron-reducing bacterium. Appl. Environ. Microbiol. 67:3750–3752.

Senn, D.B., and H.F. Hemond. 2002. Nitrate controls on iron and arsenic in an urban lake. Science 296:2373–2376.

Shelobolina, E.S., C.G. Vanpraagh, and D.R. Lovley. 2003. Use of ferric and ferrous iron containing minerals for respiration by *Desulfitobacterium frappieri*. Geomicrobiol. J. 20:143–156.

Shriver, D.F., P. Atkins, and C.H. Langford. 1994. Inorganic chemistry. W.H. Freeman and Co., New York.

Smith, M.S. 1983. Nitrous oxide production by *Escherichia coli* is correlated with nitrate reductase activity. Appl. Environ. Microbiol. 45:1545–1547.

Sorensen, J. 1982. Reduction of ferric iron in anaerobic, marine sediment and interaction with reduction of nitrate and sulfate. Appl. Environ. Microbiol. 43:319–324.

Sorensen, J., and L. Thorling. 1991. Stimulation by lepidocrocite (γ-FeOOH) of Fe(II)-dependent nitrite reduction. Geochim. Cosmochim. Acta 55:1289–1294.

Stookey, L.L. 1970. Ferrozine—A new spectrophotometric reagent for iron. Anal. Chem. 42:779–781.

Straub, K.L., M. Benz, B. Schink, and F. Widdel. 1996. Anaerobic, nitrate-dependent microbial oxidation of ferrous iron. Appl. Environ. Microbiol. 62:1458–1460.

Stucki, J.W., G.W. Bailey, and H.M. Gan. 1996. Oxidation–reduction mechanisms in iron-bearing phyllosilicates. Appl. Clay Sci. 10:417–430.

Suess, E. 1979. Mineral phases formed in anoxic sediments by microbial decomposition of organic matter. Geochim. Cosmochim. Acta 43:339–352.

Tratnyek, P.G., and N.L. Wolfe. 1993. Oxidation and acidification of anaerobic sediment–water systems by autoclaving. J. Environ. Qual. 22:375–378.

Van Bodegom, P.M., J.V. Reeven, and H.A.C. Denier Van Der Gon. 2003. Prediction of reducible soil iron content from iron extraction data. Biogeochemistry 64:231–245.

Van Cleemput, O., and L. Baert. 1983. Nitrite stability influenced by iron compounds. Soil Biol. Biochem. 15:137–140.

Weatherburn, M.W. 1967. Phenol-hypochlorite reaction for determination of ammonia. Anal. Chem. 39:971–974.

Weber, K.A., F.W. Picardal, and E.E. Roden. 2001. Microbially-catalyzed nitrate-dependent oxidation of biogenic solid phase Fe(II) compounds. Environ. Sci. Technol. 35:1644–1650.

Wehrli, B. 1990. Redox reactions of metal ions at mineral surfaces. p. 311–336. *In* W. Stumm (ed.) Aquatic chemical kinetics. John Wiley & Sons, New York.

Zachara, J.M., R.K. Kukkadapu, J.K. Fredrickson, Y.A. Gorby, and S.C. Smith. 2002. Biomineralization of poorly crystalline Fe(III) oxides by dissimilatory metal reducing bacteria (DMRB). Geomicrobiol. J. 19:179–207.